Biomacromol. J., Vol. 5, No. 2, 161-173, December 2019.

Biomacromolecular Journal
www.bmmj.org

Molecular Spectroscopy and Molecular Dynamic Simulation to Study the Binding of DNA with 3-Hydroxy-2-oxindole

F. Norouzi Rostami[a], M.R. Housaindokht[a,b,*], R. Jalal[a,b], A.A. Esmaeilli[a] and F. Janati-Fard[b]

[a]*Department of Chemistry, Faculty of Science, Ferdowsi University of Mashhad, Mashhad, Iran*

[b]*Research and Technology Center of Biomolecules, Ferdowsi University of Mashhad, Mashhad, Iran*

(Received 4 June 2020, Accepted 19 July 2020)

ABSTRACT

This study aimed to investigate the interaction between 5-(2-hydroxy-2-oxo-2,3-dihydro-1H-indol-3-yl)-1,3thiazolidine-2,4-dione (oxindole A) and DNA with and without ultrasound treatment. Absorption studies have indicated that oxindole A could bind to CT-DNA with the binding constant of 30,000 and 26,666 M^{-1} with and without ultrasound treatment, respectively. In the competitive fluorescence method, the displacement of 4′,6-diamidino-2-phenylindole (DAPI) as a probe bound to the groove, from the DNA groove occurred by oxindole A. Using the Stern-Volmer plot, quenching constant was calculated to be 1,411 and 2,753 M^{-1} with and without ultrasound, respectively. Viscometric experiments have confirmed the groove binding of oxindole A to the DNA, which is consistent with the molecular dynamic simulation. The analysis of Pi, as a measure of affinity for ligand binding, has also revealed that the DA3, DG4, DC5, DT7, DC8 and DG9 of DNA have the highest affinity toward oxindole A. In addition, the results of the cell viability assay of the DU145 cell line have demonstrated that oxindole A has cytotoxic effects.

Keywords: Interaction, CT-DNA, Oxindole, Spectroscopy, Ultrasound, Simulation

INTRODUCTION

DNA is a genetic compound responsible for vital processes, and DNA changes by any factors could modify biological processes [1]. According to the literature, some small molecules could modify, inhibit or activate the DNA function, acting as medicine by changing the features of the binding of these regulating proteins [2]. It is crucial to recognize the binding method and function of small molecules with the DNA in order to comprehend DNA-drug bindings, design new medicines, and develop chemical probes [3]. In the evaluation of the binding between DNA and drugs, attention has mostly been paid to the binding mode. Drugs bind to the DNA through covalent and non-covalent bonds. The covalent bond in the DNA is irreversible and leads to the full inhibition of complete DNA processes, thereby causing cell death [4]. On the other hand, non-covalent bonds are reversible. They have three types, including electrostatic binding (binding between the cationic groups in the drug structure and negative charge of the sugar-phosphate backbone of DNA), groove binding (direct hydrogen bonds or Van der Waals bonds with nucleic-acid bases in the major or minor groove of the DNA), and binding through intercalation between bases (drug is placed perpendicularly in two adjacent pairs of bases) [5-8].

Ultrasound has a frequency of above 20 kHz and could be used at various intensities. Some of the devices used in daily life (*e.g.*, remote controls, door openers, dental drills for scaling) produce ultrasound [9-11]. The insulation demolition of high-voltage lines also generates an electrical leak known as the corona, which leads to the ionization of the surrounding air and ultrasound production, easily recognized by the ultrasound devices that are sensitive to the frequency range of 20-100 kHz. Ultrasound exposure may affect humans, the evaluation of which could be beneficial. Ultrasound has high penetrating power and could quickly enter the biological tissues [12]. Biological tissues are exposed to chemical and physical impacts when exposed to ultrasound [13]. Studies have indicated that various ultrasound intensities and powers exert variable effects on the DNA and cells, thereby leading to DNA synthesis

*Corresponding author. E-mail: housain@um.ac.ir

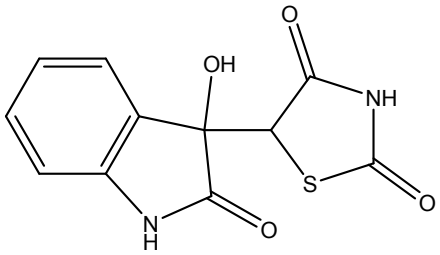

Fig. 1. The structure of 5-(2-hydroxy-2-oxo-2,3-dihydro-1H-indol-3-yl)-1,3 thiazolidine-2,4-dione.

[14,15], DNA transfer [16,17], induction of apoptosis and cancer treatment [18-23] and changes in the gene expression and promoters [24-28].

The 3-hydroxy-2-oxindole compounds have various biological and medicinal activities, such as anticancer, anti-HIV, and antioxidant functions [29]; these properties are based on various substrates in the basic three-position of 3-hydroxy-2-oxindole [30]. Molecular dynamic (MD) simulation in combination with molecular docking has numerous applications in the studies regarding ligand-macromolecule interactions [31-37].

The present study aimed to investigate the interactions between the synthesized compound of 5-(2-hydroxy-2-oxo-2,3-dihydro-1H-indol-3-yl)-1,3thiazolidine-2,4-dione (oxindole A) (Fig. 1) and DNA in the absence and presence of ultrasound using the spectroscopy and computational methods. Furthermore, the cytotoxic effects of oxindole A on the DU145 prostate cancer cell line were determined using the (3-(4,5-dimethylthiazol-2-yl)2,5-diphenyltetrazolium bromide (MTT) assay.

MATERIALS AND METHODS

Materials

All the chemicals used for DNA extraction were purchased from Merck, Germany (except phenol). Tris-saturated phenol was purchased from Denazist, and DAPI and MTT were purchased from Denazist and Sigma, respectively. The 5-(2-hydroxy-2-oxo-2,3-dihydro-1H-indol-3-yl)-1,3thiazolidine-2,4-dionewas compound was synthesized based on the research by Thakur *et al*. [38]. All the experiments involving the interactions of oxindole A with the DNA were carried out in the Tris-HCl buffer (10 mM, pH 7.4).

DNA Extraction

DNA was extracted from the thymus calf tissue (CT-DNA) using the phenol-chloroform extraction method, dissolved in cold deionized water, and preserved at the temperature of -20°C. The lack of DNA contamination was determined by assessing the absorption ratio at specific wavelengths. In this regard, the absorption ratio was considered within the range of 260-280 nm; if above 1.8, the lack of protein contamination of the extracted DNA was deduced. Within the absorption ratio range of 260-230 nm, the values above 2 were interpreted as the lack of phenol contamination of the DNA. The obtained ratios of the extracted DNA were 1.92 and 2.25, respectively, which indicated the purity of the extracted DNA. Moreover, the DNA concentration was obtained using a nanodrop spectrophotometer and estimated per each nucleotide [39]. In order to evaluate the effects of ultrasound in the tests, the DNA solution was exposed to ultrasound with the frequency of 20 kHz for 10 min before each test using the Scientz-IID Ultrasonic device.

Absorbance Measurement

The concentration of oxindole A was constant (15.2 μM), while the DNA concentration was within the range of 0-226 μM. The UV spectra were recorded within the range of 220-300 nm in the Tris-HCl buffer using the Shimadzu UV-2550 spectrophotometer. Furthermore, the effects of ultrasound on the interactions of oxindole A and DNA were evaluated after the ultrasound treatment of the DNA solution using a probe (20 kHz) for 10 min, followed by designing a similar test to the previous stage.

Fluorescence Measurements

The fluorescence measurements were carried out using

the Shimadzu FP6200 spectrofluorometer, and the competitive experiments were performed using DAPI as an intercalator probe. In order to attain the appropriate DNA concentration in the experiments, the fluorescence spectra of DAPI were initially recorded after the addition of a successive fixed amount of DNA to the DAPI solution. Afterwards, various concentrations of oxindole A (20-151 μM) were added to the DNA-DAPI mixture to evaluate its impact on the emission spectrum. Following that, the effects of ultrasound on the interactions of oxindole A and DNA were investigated using the mentioned method after the ultrasound treatment of the DNA solution with the 20 kHz probe for 10 minutes.

Viscosity Measurements

The viscosity experiments were carried out using the Ostwald viscometer (Schott Duran) at two temperatures of 35.5 °C and 65 °C.The CT-DNA concentration was fixed at 9.25 μM, while the concentration of oxindole A was variable (ri = [oxindole A]/[CT-DNA] = 0.06-1.44), and the flow time was measured using a digital stop watch. The mean values of three replicated viscosity measurements were used for the assay of the samples ($\eta/\eta_0 = t/t_0$), and η_0 and η were the relative viscosity of the DNA in the absence and presence of oxindole A, respectively. The data were presented as η/η_0 *versus* [oxindole A]/[DNA]. After exposing the DNA solution to ultrasound using the 20 kHz probe for 10 min, a similar test was designed to measure the viscosity of the solutions.

Molecular Dynamics Simulation

The initial structure of the double-stranded DNA was obtained using the 1DSC code [40], and the MD simulations were carried out using GROMACS 2019.1 with the standard CHARMM27 force-field for the DNA [41-43]. The force-field parameters and geometry of the ligand were generated using SwissParam as the force-field generation tool for small molecules [44]. Two boxes were initially prepared; the first one was with DNA, and the second box was with DNA and ligand. Afterwards, the simulation boxes were filled with the TIP3P model of water [45]. The solvated system was neutralized by adding sodium ions to the simulation box, and energy minimization was performed using the steepest descent method, followed by the conjugate gradient method. In the first step of the MD simulation (equilibrium), the solute (DNA, counter ion, and ligand) was fixed, and the position-restrained dynamics simulation of the system proceeded at the temperature of 300 K. The periodic boundary condition was used, along with the leapfrog algorithm (time step: 2 fs). At the next stage, the MD simulation of each system (100 ns) was performed at the temperature of 300 K and pressure of one bar.

MTT Assay

The MTT assay was used to evaluate the cytotoxic effects of oxindole Aon the cellular genome of human prostate cancer. The test was carried out in 48 hours, and the cells were cultured in a 96-well plate. In this assay, untreated cells (control) and cells treated with oxindole A (25-200 μM) were applied. Initially, 200 μM of the cellular suspension containing 3,200 cells (104 cell per each cm^2) was poured into each well of the plate. After incubation for 24 h, the above surface of the cells was replaced with the new culture (200 μl) containing oxindole A with the concentrations of 25-200 μM, followed by the incubation of the combination. The MTT assay was performed for 48 h after the treatment. To this end, 20 μl of the MTT solution was added to each well, and the plate was incubated for four hours. Afterwards, the medium containing the treated solution and the remaining MTT stain was removed from each well. Following that, 150 μl of dimethylsulfoxide was added, and the absorption of the samples was read at 570 nm using the enzyme-linked immunosorbentassay (ELISA) microplate reader (ELX800G of Bio-TekInstruments Inc.).

RESULTS AND DISCUSSION

The interaction of oxindole A with DNA was assessed using UV spectroscopy in order to identify the possible binding mode to the DNA and determine the binding constant to CT-DNA (K_b). The absorption spectrum of oxindole A was also evaluated in the absence and presence of various DNA concentrations in two modes of exposed and non-exposed to ultrasound (Fig. 2). The absorption intensity of the spectrum of oxindole A increased with the addition of DNA to the oxindole A solution, which is

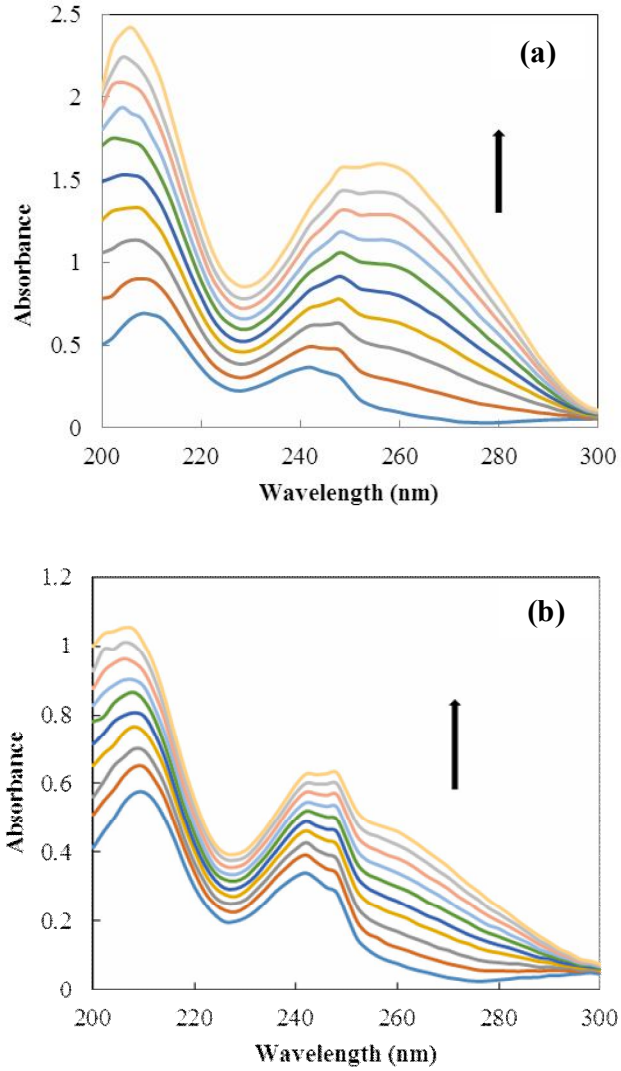

Fig. 2. The absorption spectra of oxindole A (15.2 µM) in the presence of different concentrations of CT-DNA (50.8-226 µM), a) without and b) with ultrasound treatment, from bottom to the top.

referred to as hyperchromesis; the increase was indicative of electrostatic interaction to CT-DNA [46].

In order to obtain the binding constant of the interaction between oxindole A and CT-DNA, the half-reciprocal equation (Eq. (1)) was used, as follows:

$$\frac{[DNA]}{(\varepsilon_a - \varepsilon_f)} = \frac{[DNA]}{(\varepsilon_b - \varepsilon_f)} + \frac{1}{K\,(\varepsilon_b - \varepsilon_f)} \quad (1)$$

Where [DNA] is the DNA concentration, ε_a is the apparent molar absorption coefficient, which was estimated by A_{obsd}/[oxindoleA], and ε_f and ε_b show the molar absorption coefficient of the free and bounded oxindole A, respectively. In the equation above, $1/\Delta\varepsilon$ and K_b could be estimated from the plot of [DNA]/(ε_b - ε_f) *vs.* [DNA], and the slope of the plot was equal to K_b [46,47].

Figure 3 shows the plot of [DNA]/(ε_b - ε_f) against [DNA] with and without the ultrasound treatment. The binding constant of oxindole A to CT-DNA was 30,000 and 26,666 M^{-1} with and without ultrasound,

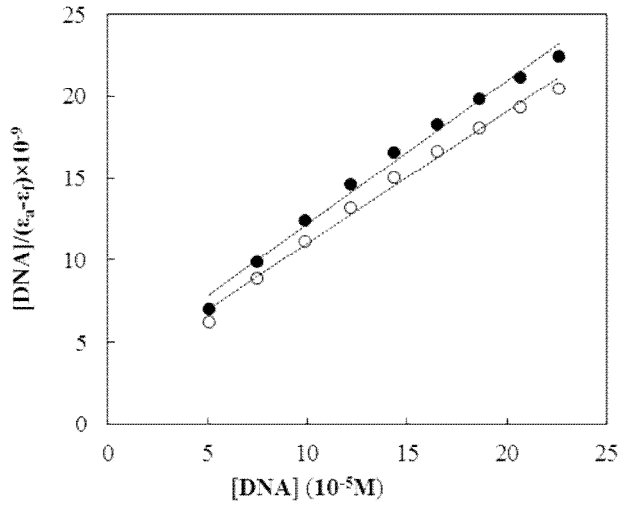

Fig. 3. Plots of [DNA]/(ε_b . ε_f) *vs*. [DNA] for determining binding constant in 242 nm, ○) without and ●) with ultrasound treatment.

respectively. With regard to the binding constant of Tris (1,10-phenanthroline)ruthenium(II), which is a compound that binds to the groove [48], and based on the other compounds that bind to the DNA groove, including 3-(pyridine-2-yl)-5,6-diphenyl-as-triazine (8.62×10^3 M^{-1}) [49], [(Py-3')TPP-Ru(phen)$_2$Cl]Cl (1.35×10^5 M^{-1}), [Ni(Py-3')TPP-Ru(phen)$_2$Cl][PF_6] (1.29×10^5 M^{-1}), [Cu(Py-3')TPP-Ru(phen)$_2$Cl](PF_6) (1.22×10^5 M^{-1}) [50], [Nd(phen)$_2$$Cl_3$.$OH_2$] ($6.76 \times 10^4$ M^{-1}) and [Pr(phen)$_2$$Cl_3$.$OH_2$] ($1.83 \times 10^4$ M^{-1}) [51], it seems that oxindole A in the current research bound to CT-DNA through the DNA grooves. The comparison of the binding constants with and without the ultrasound treatment showed that the ultrasound had no significant effect on the binding constant, and both modes of oxindole A were able to bind to the DNA grooves.

Fluorescence Studies (Competitive Binding with DAPI)

In order to investigate the interaction mode between the compound and DNA, a competitive fluorescence experiment was performed using DAPI as a known fluorogenic probe that binds to the minor groove of the DNA to evaluate the type of the interaction between the drugs and DNA [52]. As is observed in Fig. 4, the concentration of the applied DNA was determined at 0.88 mM.

The evaluation of the competitive fluorescence between oxindole A and DAPI indicated that the emission intensity of DAPI and DNA decreased without the ultrasound treatment with the addition of various concentrations of oxindole A (Fig. 5). The reduction may be due to the displacement of DAPI from the DNA groove by the competitive compound. Using the Stern-Volmer plot, quenching constant of DNA molecule was calculated by the following equation (Eq. (2))

$$\frac{F_0}{F} = 1 + K_{SV}[Q] \quad (2)$$

Where F_0 and F are the fluorescence intensity in the absence and presence of DNA, respectively, K_{sv} is the quenching constant of the Stern-Volmer plot, and [Q] is the concentration of the quenching factor. By using the Stern-Volmer plot [53], the quenching constant was estimated to be 2.7535×10^3 M^{-1} for the competitive experiment without the ultrasound treatment (Fig. 6). However, the quenching constant in the competitive fluorescence test between oxindole A and DAPI was consistent with those of the other compounds [6,8,54-56].

The investigation of the effects of ultrasound on the emission spectra of DAPI-DNA showed that the increased

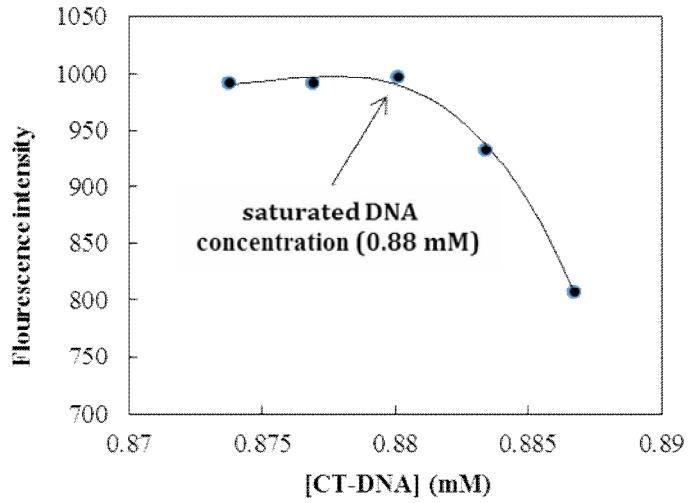

Fig. 4. Fluorescence intensity against the different concentrations of CT-DNA and constant concentration of DAPI (30 µM).

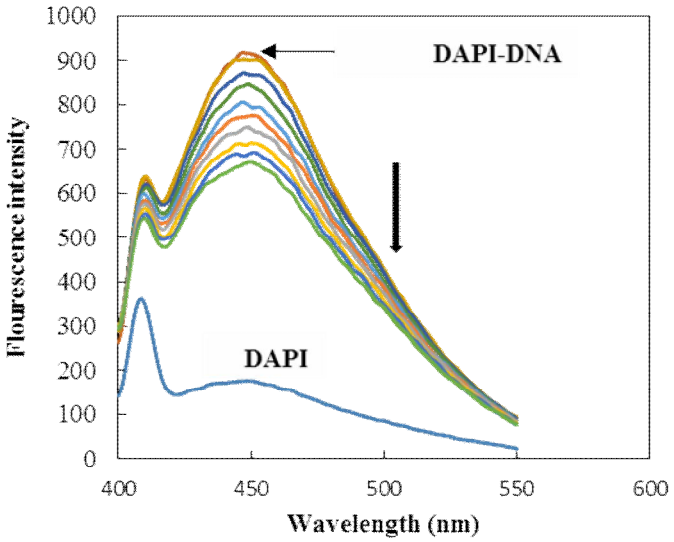

Fig. 5. Emission spectra of the DAPI-DNA complex in the absence of ultrasound with increasing various concentration of oxindole A (20- 151.3 µM) in Tris-HCl buffer. The concentrations of DAPI and DNA were 30 µM and 0.88 mM, respectively. The arrow shows the change in emission intensity by increasing the concentration of oxindole A.

concentration of oxindole A reduced the intensity of the emission (Fig. 7). The reduction could be due to the displacement of DAPI from the DNA groove by the oxindole A. The quenching constant was estimated to be $1.4113 \times 10^3\ M^{-1}$ in the presence of the DNA exposed to ultrasound (Fig. 8). Therefore, it was observed that the

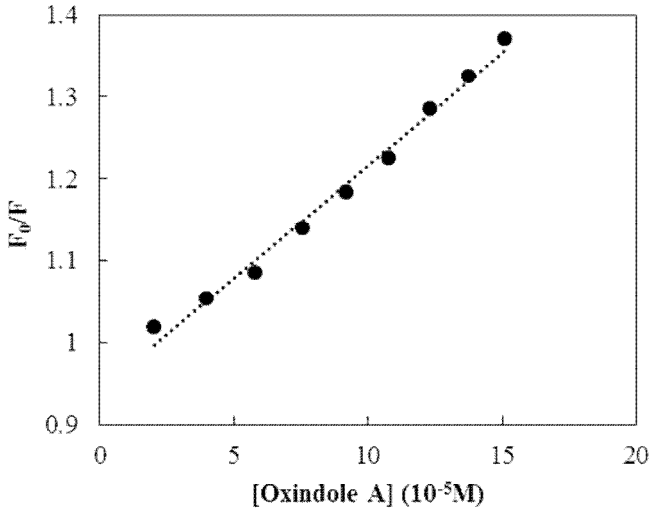

Fig. 6. Stern-Volmer plot for determining quenching constant of oxindole A without ultrasound treatment.

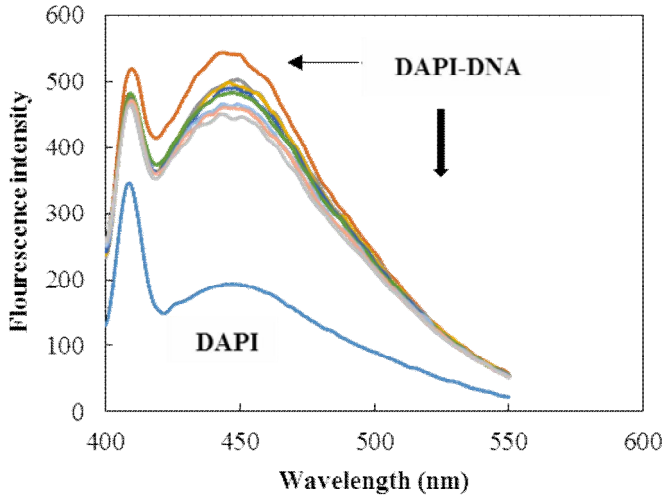

Fig. 7. Emission spectra of the DAPI-DNA complex in the presence of ultrasound with increasing various concentration of oxindole A (20-151.3 µM) in Tris-HCl buffer. The concentrations of DAPI and DNA were 30 µM and 0.88 Mm, respectively. The arrow shows the change in emission intensity by increasing the concentration of oxindole A.

ultrasound reduced the quenching constant.

Viscosity Measurements

Viscosity measurement of the DNA solution in the presence of compounds is an essential test for determining the binding mode of the DNA [57]. Intercalation molecules could increase the length of double-stranded DNA by placing the compounds between the base pairs, which increases DNA viscosity [58]. Meanwhile, the compounds that exclusively bind to the DNA groove via non-classic and

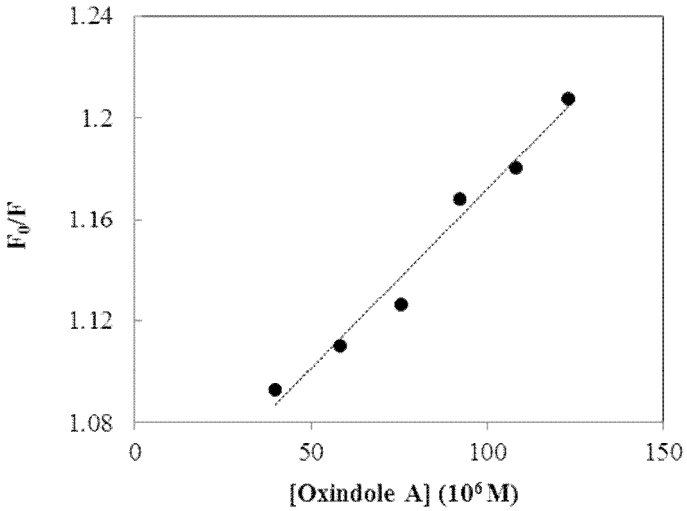

Fig. 8. Stern-Volmer plot for determining quenching constant of oxindole A with ultrasound treatment.

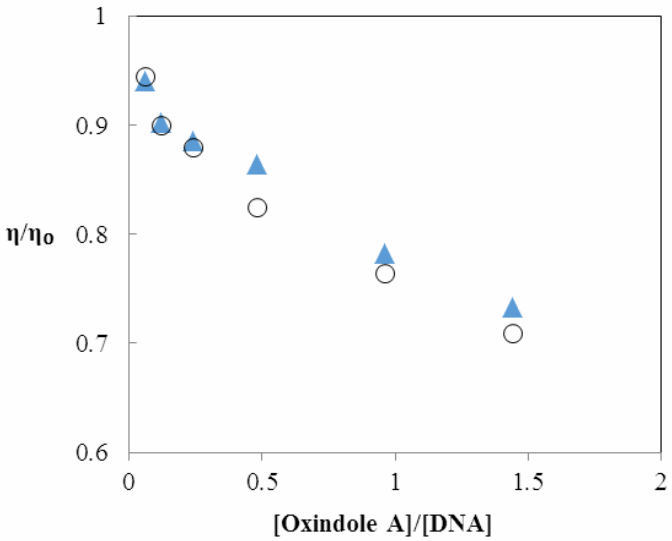

Fig. 9. Effect of increasing amounts of oxindole Aon the relative viscosities of CT-DNA (9.25 µM) in temperature of 35.5°C, ○) without and Δ) with ultrasound treatment) in Tris-HCl buffer.

inconsiderable binding often reduce viscosity or make no changes in the viscosity of the DNA solution. Relatively small changes in the DNA viscosity is indicative of weak binding to the DNA, which corresponds to DNA groove binding [59]. Figure 9 depicts the plot of (η/η0) *vs.* [compound]/[CT-DNA] in the absence and presence of various concentrations of oxindole A at the temperature of 35.5 °C. According to our finding, the viscosity of the CT-DNA solution decreased in the presence of various concentrations of oxindole A. This behavior is highly likely to the other compounds which could bind to the groove, such as adefovirdipivoxil [59] and hexaazamacrocyclic copper(II) [60]. Therefore, this method could show the binding to the DNA groove in confirmation of other

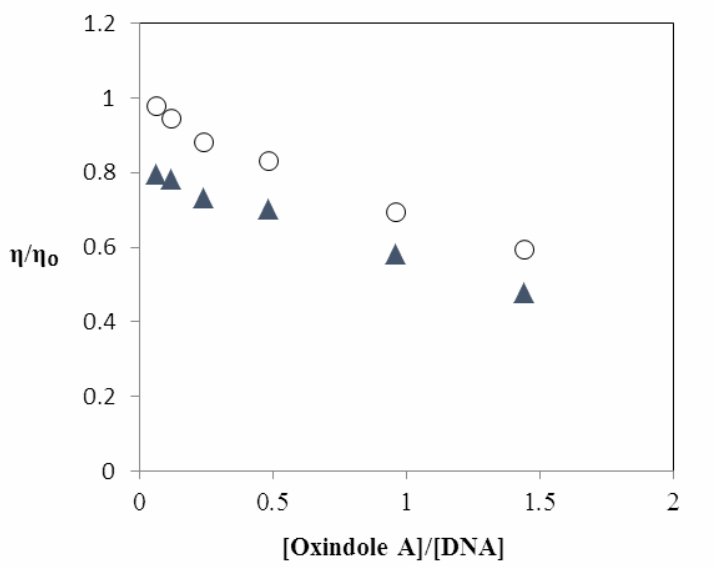

Fig. 10. Effect of increasing amounts of oxindole A on the relative viscosities of CT-DNA (9.25 μM) in temperature of 65 °C, (○without and Δ with ultrasound treatment) in Tris-HCl buffer.

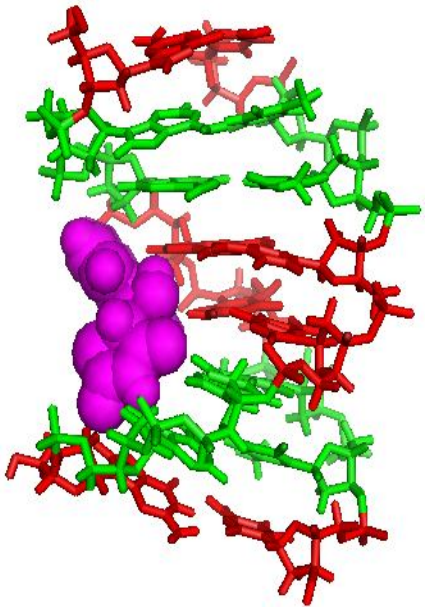

Fig. 11. The FEL analysis for DNA (DG-DC and DA-DT were represented by red and green, respectively) in the presence of oxindole A (purple) during 100 ns MD simulation.

techniques.

Figure 10 showed a more significant reduction in relative viscosity in the presence of oxindole A in the DNA not exposed to ultrasound. In other words, DNA exposure to ultrasound resulted in the less significant increase in the DNA length.

Table 1. Nucleotidein DNA with the Value of Pi in DNA-oxindole A System

Nucleotide in DNA	Pi values	Nucleotide in DNA	Pi values
DG1	0.7189	DG9	2.5866
DA2	0.2161	DA10	0.7525
DA3	1.0908	DA11	0.4110
DG4	1.6530	DG12	0.2490
DC5	1.3798	DC13	0.3793
DT6	0.9529	DT14	0.6820
DT7	1.1817	DT15	0.6208
DC8	2.3906	DC16	0.8342

Cytotoxicity Assay

To investigate the viability of the cells in 48 h after the treatment, the MTT assay was performed in triplicate [61,62]. According to the MTT results, oxindole A (200 μM) had significant antiproliferative effects on the DU145 prostate cancer cells after 48 hours of treatment ($P < 0.05$).

Molecular Dynamics Results

The MD calculation was performed on the DNA in the absence and presence of oxindole A using the GROMACS software. The free energylandscape (FEL) provides an insight into the ligand-macromolecule interactions throughidentifying the structural changes of the macromolecule during interactions [63,64]. Moreover, the FEL analysis provides beneficial information about the relation between the structure, dynamics, and stability of a macromolecule [65]. The FEL can recognize the most stable conformation of a biomolecule in simulation conditions [66,67].

In the present study, the FEL analysis was applied to determine the most stable conformation of the simulated systemsduring the MD simulation (Fig. 11). As is shown in Fig. 11, the most stable conformations of the DNA in the presence of oxindole confirmed the major groove binding of oxindole A to the DNA. However, the results of the MD simulation indicated DNA groove binding, which is in line with the results of experimental studies.

Due to the motions of the ligand and protein, the ligand could collide with different parts of the protein. To assess the binding site of the ligands to the DNA using the MD simulation, the collisions of ligand with each nucleotide of the DNA were evaluated initially. Following that, the average number of the collisions with each nucleotide was estimated. The measure of the affinity of a nucleotide (Pi) referred to a conformational factor, toward a ligand, which was also assessed in our study. A residue could be in different toward the ligand when the Pi value turns out to be unity. The nucleotide i with $Pi > 1$ is supposed to have an affinity toward the ligand, while with $Pi < 1$, it has no affinity [68,69]. Table 1 shows the Pi values for the nucleotide of DNA in the binary and ternary systems. The obtained results revealed that DA3, DG4, DC5, DT7, DC8, and DG9 of the DNA had the largest Pi value, which indicated the greatest affinity toward the ligand in the DNA-oxindole A system.

CONCLUSIONS

In the current research, the interaction of the calf thymus DNA (CT-DNA) with oxindole A was investigated using UV absorption, fluorescence spectroscopy, viscometry, and MD simulation. UV absorption demonstrated that hyperchromism occurred by adding various DNA

concentrations to a constant concentration of oxindole A. The binding constants for oxindole A with exposed and non-exposed DNA to ultrasound were 26×10^3 and 30×10^3 M^{-1}, respectively. The results of fluorescence spectroscopy confirmed the predicted interaction model with the UV method, and the quenching constants were calculated to be 2.75×10^3 and 1.41×10^3 M^{-1} without and with ultrasound treatment, respectively. The small changes in the DNA viscosity by adding the compound showed the weak binding to the DNA, which confirmed the binding to the DNA groove. Furthermore, viscosity experiments demonstrated that DNA exposure to ultrasound resulted in the less significant increase of the DNA length. The MD simulation predicted binding to the major groove of DNA with oxindole A, which is in congruence with the results of the experimental studies. The results regarding the Pi value demonstrated that DA3, DG4, DC5, DT7, DC8 and DG9 of the DNA had the largest values. According to the results of the MTT assay, the most significant anti-reproduction effect of oxindole A on the DU145 cells was observed at the concentration of 200 µM after 48 hours of treatment.

ACKNOWLEDGEMENTS

This research was supported by Ferdowsi University of Mashhad, Iran (Grant P/15764-89/9/13).

REFERENCES

[1] Z. Song, H. Wang, B. Ren, B. Zhang, Y. Hashi, S. Chen, J. Chromatogr. A 1282 (2013) 102.

[2] S.A. Shaikh, S.R. Ahmed, B. Jayaram, Arch. 429 (2004) 81.

[3] C. Ozluer, H.E.S. Kara, J. Photochem. Photobiol. 138 (2014) 36.

[4] P.C. Billings, R.J. Davis, B.N. Engelsberg, K.A. Skov, E.N. Hughes,Biochem. Biophys. Res. Commun. 188 (1992) 1286.

[5] A. Silvestri, G. Barone, G. Ruisi, D. Anselmo, S. Riela, V.T. Liveri, J. Inorg. Biochem. 101 (2007) 841.

[6] T. Zhao, S. Bi, Y. Wang, T. Wang, B. Pang, T. Gu, Spectrochim. Acta. A 132 (2014)198.

[7] M. Khorasani-Motlagh, M. Noroozifar, S. Khmmarnia, Spectrochim. Acta. A 78 (2011) 389.

[8] S. Shahraki, H. Mansouri-Torshizi, Z. Ghanbari, A. Divsalar, A.-A. Saboury, Biomacromol. J. 3 (2017) 60.

[9] G. Zhang, P. Fu, J. Pan, J. Lumin. 134 (2013)303.

[10] F.A. Duck, Prog. Biophys. Mol. Biol. 93 (2007)176.

[11] Y. Zou, P. Xu, H. Wu, M. Zhang, Z. Sun, C. Sun, D. Wang, J. Cao, W. Xu, Int. J. Biol. Macromol. 113 (2013) 640.

[12] A. Amiri, P. Sharifian, N. Soltanizadeh, Int. J. Biol. Macromol. 111 (2018) 139.

[13] X. Wang, L.-L. He, B. Liu, X.-F. Wang, L. Xu, T. Sun, Int. J. Biol. Macromol. 120 (2018) 1865.

[14] M.H. Ali, K.A. Al-Saad, C.M. Ali, Phys. Med. 30 (2014) 221.

[15] S. Heyner, V. Abraham, M. Wikarczuk, M. Ziskin, Mol. Reprod. Dev. 25 (1990) 09.

[16] W.A. Elmer, A.C. Fleischer,J. Clin. Ultrasound. 2 (1974) 191.

[17] 16] V.G. Zarnitsyn, M.R. Prausnitz,Ultrasound. Med. Biol. 30 (2004) 527.

[18] Y. Qiu, C. Zhang, J. Tu, D. Zhang, J. Biomech. 45 (2012) 1339.

[19] L. Forýtková, I. Hrazdira, V. Mornstein, Ultrasound. Med. Biol. 21 (1995) 585.

[20] M.G. Andreassi, L. Venneri, E. Picano, Prog. Biophys. Mol. Biol. 93 (2007) 399.

[21] H. Tsuru, H. Shibaguchi, M. Kuroki, Y. Yamashita, M. Kuroki, Free. Radic. Biol. Med. 53 (2012) 464.

[22] L.B. Feril Jr, T. Kondo, Int. Corros. Conf.Ser. 1274 (2004) 133.

[23] M.A. Hassan, L.B. Feril Jr, K. Suzuki, N. Kudo, K. Tachibana, T. Kondo, Ultrason. Sonochem. 16 (2009) 372.

[24] W. Hiraoka, H. Honda, L.B. Feril Jr, N. Kudo, T. Kondo, Ultrason. Sonochem. 13 (2006) 535.

[25] X.-H. Li, P. Zhou, L.-H. Wang, S.-M. Tian, Y. Qian, L.-R. Chen, P. Zhang, Ultrasonics. 52 (2012) 186.

[26] N.A. Geis, C.R. Mayer, R.D. Kroll, S.E. Hardt, H.A. Katus, R. Bekeredjian, Ultrasound. Med. Biol. 35 (2009) 1119.

[27] R. Ogawa, A. Morii, A. Watanabe, Z.-G. Cui, G. Kagiya, T. Kondo, N. Doi, L.B. Feril Jr, Ultrason. Sonochem. 20 (2013) 460.

[28] R. Ogawa, S.-i. Lee, H. Izumi, G. Kagiya, T. Yohsida, A. Watanabe, A. Morii, S. Kakutani, T. Kondo, L.B. Feril Jr, Ultrason. Sonochem. 16 (2009) 379.
[29] H. Hosseinkhani, Y. Tabata, J. Control. Release 108 (2005) 540.
[30] S.V. Vuppalapati, Y.R. Lee, Tetrahedron. 68 (2012) 8286.
[31] G.M. Ziarani, P. Gholamzadeh, N. Lashgari, P. Hajiabbasi, J. Org. Chem. 1 (2013) 470.
[32] H. Monhemi, M.R. Housaindokht, A. Nakhaei Pour, J. Phys. Chem. B 119 (2015) 10406.
[33] F. Janati-Fard, M.R. Housaindokht, H. Monhemi, J. Mol. Liq. 134 (2016) 16.
[34] F. Cui, Q.Liu, H. Luo, G. Zhang, J. Fluoresc. 24 (2014) 189.
[35] P. Akhshi, G. Acton, G. Wu, J. Phys. Chem. B 116 (2012) 9363.
[36] S. Pal, S. Paul, Int. J. Biol. Macromol. 121 (2019) 350.
[37] D. Ajlooa, S. Shabanpanah, B. Shafaatian, M. Ghadamgahi, Y. Alipour, T. Lashgarbolouki, A.A. Saboury, Int. J. Biol. Macromol. 77 (2015) 193.
[38] D. Ajloo, M. EslamiMoghadam, A.A. Saboury, Kh. Ghadimi, M. Ghadamgahi, A. Divsalar, M. Sheikh Mohammadi, Kh. Yousefi, Inorganica. Chim. Acta 430 (2015) 144.
[39] P.B. Thakur, H.M. Meshram, RSC. Advances 4 (2014) 5343.
[40] A. Fleck, D. Begg, Biochim. Biophys. Acta 108 (1965) 333.
[41] F. Vahdati Rad, M.R. Housaindokht, R. Jalal, H.E. Hosseini, A.V. Doghaei, S.S. Goghari, J. Fluoresc. 24 (2014) 1225.
[42] M.J. Abraham, T. Murtola, R. Schulz, S. Páll, J.C. Smith, B. Hess, E. Lindahl, Software X. (2015) 19.
[43] A.D. MacKerell, N. Banavali, N. Foloppe, Biopolymers. 56 (2000) 257.
[44] T. Sun, A. Mirzoev, N. Korolev, A.P. Lyubartsev, L. Nordenskiöld, J. Phys. Chem. B 121 (2017) 7761.
[45] V. Zoete, M.A. Cuendet, A. Grosdidier, J. Comput. Chem. 32 (2011) 2359.
[46] W.L. Jorgensen, J. Chandrasekhar, J.D. Madura, R.W. Impey, M.L. Klein, J. Chem. Phys. 79 (1983) 926.
[47] S. Tabassum, S. Parveen, F. Arjmand, Acta. Biomater. 1 (2005) 677.
[48] E. Ramachandran, P. Kalaivani, R. Prabhakaran, M. Zeller, J.H. Bartlett, P.O. Adero, T.R. Wagner, K. Natarajan, Inorg. Chim. Acta 385 (2012) 94.
[49] B. Pedras, R.M. Batista, L. Tormo, S.P. Costa, M.M.M. Raposo, G. Orellana, J.L. Capelo, C. Lodeiro, Inorg. Chim. Acta 381 (2012) 95.
[50] X.-L. Wang, H. Chao, H. Li, X.-L. Hong, Y.-J. Liu, L.-F. Tan, L.-N. Ji, J. Inorg. Biochem. 98 (2004) 1143.
[51] Y. Liu, T. Chen, Y.-S. Wong, W.-J. Mei, X.-M. Huang, F. Yang, J. Liu, W.-J. Zheng, Chem. Biol. Interact. 183 (2010) 349.
[52] M. Khorasani-Motlagh, M. Noroozifar, S. Mirkazehi-Rigi, Spectrochim. Acta A 79 (2011) 978.
[53] A. Basu, G.S. Kumar, Int. J. Biol. Macromol. 62 (2013) 257.
[54] N. Li, Y. Ma, C. Yang, L. Guo, X. Yang, Biophys. Chem. 116 (2005) 199.
[55] N. Shahabadi, S. Amiri, Spectrochim. Acta A 138 (2015) 840.
[56] X. Zhou, G. Zhang, L. Wang, Int. J. Biol. Macromol. 67 (2014) 228.
[57] M. Khorasani-Motlagh, M. Noroozifar, S. Mirkazehi-Rigi, Spectrochim. Acta A 75 (2010) 598.
[58] M.N. Patel, C.R. Patel, H.N. Joshi, K.P. Thakor, Spectrochim. Acta A 127 (2014) 261.
[59] C. Icsel, V.T. Yilmaz, J. Photochem. Photobiol. B 130 (2014)115.
[60] N. Shahabadi, M. Falsafi,Spectrochim. Acta. A 125 (2014) 154.
[61] J. Liu, T. Zhang, T. Lu, L. Qu, H. Zhou, Q. Zhang, L. Ji, J. Inorg. Biochem. 91 (2002) 269.
[62] [61] T. Mosmann, J. Immunol. Methods. 65 (1983) 55.
[63] Y. Liu, D.A. Peterson, H. Kimura, D. Schubert, J. Neurochem. 69 (1997) 581.
[64] D. Leva, F.S., Novellino, E. Cavalli, A. Parrinello, M. Limongelli, Nucleic. Acids. Res. 42 (2014) 5447.
[65] K. Moritsugu, T. Terada, A. Kidera, J. Phys. Chem. B 121 (2017) 731.
[66] F. Moghaddasi, M.R. Housaindokht, M. Darroudi,

M.R. Bozorgmehr, A. Sadeghi, J. Mol. Liq. 264 (2018) 242.
[67] K.M. ElSawy, Adv. Phys. Org. Chem. 3 (2016) 1.
[68] R. Karamzadeh, M.H. Karimi-Jafari, A. Sharifi-Zarchi, H. Chitsaz, G.H. Salekdeh, A.A. Moosavi-Movahedi, Sci. Rep. 7 (2017) 3666.
[69] M.R. Housaindokht, M.R. Bozorgmehr, M. Bahrololoom, J. Theor. Biol. 254 (2008) 294.
[70] F.S. Mohseni-Shahri, M.R. Housaindokht, M.R. Bozorgmehr, A.A. Moosavi-Movahedi, J. Solution. Chem. 45 (2016) 265.